

PARAMETER PLANE ANALYSIS OF FORCED  
NONLINEAR OSCILLATIONS\*

D. Šiljak\*\*

J. Moore\*\*\*

Summary. This paper presents an application of the parameter plane method to the analysis of forced oscillations and jump-resonance phenomena in nonlinear systems subject to periodic forcing signals. The approximate analysis procedure utilizes the describing function technique. The advantage of the procedure lies in the fact that only one parameter plane diagram is necessary to investigate the effects of different forcing signals. If the amplitude of the forcing function is fixed, a modification of the proposed procedure enables an analysis of the jump-resonance phenomena for different nonlinear characteristics. The stability and sensitivity of forced nonlinear oscillations are also discussed.

The procedure is illustrated by examples.

INTRODUCTION

So far, mostly free nonlinear oscillations were considered in the parameter plane [1-4], and the right side of differential equations describing the systems was identically equal to zero. The only cases when an external forcing signal was present have been analyzed in reference [4] in connection with asymmetrical oscillations. The analysis, however, was performed under the assumption that the external forcing function is either constant or a slow-varying function of time with respect to the corresponding periodic solution. In other words,

---

\* The research reported herein was supported by the National Aeronautics and Space Administration under Grant No. NGR 05-017-010. The paper has been presented at the Fourth Allerton Conference on Circuit and System Theory, University of Illinois, Monticello, Ill., October 5-7, 1966.

\*\*D. Šiljak is with the Electrical Engineering Department, University of Santa Clara, Santa Clara, California.

\*\*\*J. Moore is with the Department of Electrical Engineering, University of Newcastle, New South Wales, Australia.

(THRU)	(CODE)	(CATEGORY)
N 68-33685	27	10
(ACCESSION NUMBER)	(PAGES)	(NASA CR OR TMX OR AD NUMBER)
CF-89189		
FACILITY FORM 602		

CFSTI H.C.  
M.F.

the frequency of the external signal has been sufficiently lower than the frequency of the existing limit cycle. This assumption greatly simplified the analysis and gave rise to useful practical applications.

When no restrictions are imposed on the frequency of the external signal, the oscillations can become complex even in the case of second-order systems [5-7]. Several new phenomena can occur which could not take place in a free nonlinear system. In this section, however, attention will be focused on the jump resonance phenomena which is of importance in a number of nonlinear engineering problems.

The jump resonance phenomena in high-order nonlinear systems has been long under consideration in connection with the evaluation of the closed-loop frequency response of feedback control systems containing a nonlinearity [8-20]. These methods exclusively apply the describing function technique. This application of the describing function to nonautonomous systems has been based upon intuition and remained suspected until recently when the more exact conditions under which such application is correct have been developed [21-24].

The methods of Levinson [8] and Prince [9] involve the definition of an equivalent gain which approximates the given nonlinear characteristic. The methods are convenient for certain single-valued limiting nonlinearities, but can hardly be adapted for more complicated nonlinear characteristics. This concept, however, has been successfully extended by Booton [25] to nonlinear systems with stochastic signals. West and others [10,15] applied the dual-input describing function to determine the condition of the jump resonance to take place in systems with a polynomial nonlinearity. The

extension to other kinds of nonlinearities is limited by the labor involved in calculating the corresponding dual-input describing function. Ogata and Hopkin's analytic techniques [11,13] are limited to relay characteristics, or, perhaps, saturating nonlinearities, since the output wave shape of the nonlinearity should be assumed. Considerable work is required to make a proper assumption in cases other than the ideal relay characteristic. Stein and Thaler [12] proposed a trial-and-error procedure to calculate the closed-loop frequency response by using the Nichols chart. A similar concept has been used with some modifications in reference [17] by McAllister.

The idea of finding conditions under which the jump resonance occurs and then designing the linear part of the system to avoid that as proposed by West and others [10] has been successfully applied along with the common describing function in references [15,16,18]. The methods, however, cannot give an insight into the frequency response of the closed loop systems. Moreover, the procedures are extremely cumbersome when applied to the simplest multi-valued nonlinearities or nonlinearities with the frequency dependent describing functions.

The frequency response can be analyzed by a different approach proposed by Gibson [19], which has some apparent advantages over the previously presented procedures. It enables information to be readily obtained about the effects on the frequency response of varying the nonlinear parameters. In addition, it does not require the analytical expression of the describing function and can thus be applied to experimentally obtained data. The procedure, however, has to be repeated each time the amplitude of the forcing periodic signal is changed. This can be circumvented by the technique of Popov and Palitov [14]

at the expense that the nonlinearity cannot be varied without recalculating all the necessary curves.

In this paper, the separate ideas of the references mentioned in the preceding paragraph will be employed using the parameter plane concept. The proposed analysis is directed towards the consideration of jump phenomena in high-order nonlinear systems. In addition, the stability and sensitivity of the periodic oscillations is briefly discussed on the basis of reference [3].

Periodic Solutions. Jump-Resonance.

Consider again the nonlinear differential equation

$$B(s)x + C(s) F(x, sx) = H(s)f, \quad s \equiv \frac{d}{dt} \quad (1)$$

where, at the right hand side, the forcing function  $f = f(t)$  is

$$f = A_f \sin (\Omega_f t - \varphi) \quad (2)$$

and  $B(s)$ ,  $C(s)$ , and  $H(s)$  are polynomials in  $s$ .  $C(s)$  and  $H(s)$  are polynomials with degrees less than that of the polynomial  $B(s)$ . The function  $F(x, sx)$  represents the nonlinearity. The basic problem is to determine the conditions under which equation (1) has a periodic solution  $x = x(t)$  sufficiently close to

$$x = A \sin (\Omega_f t) \quad (3)$$

where the frequency  $\Omega_f$  is the known frequency of the forcing function  $f(t)$  in

(2); and then to evaluate the unknown values of the amplitude  $A$  and the phase-shift  $\varphi$ .

By a suitable transformation, the above problem can be reduced to that of free symmetrical oscillations considered in references [1-3]. To do this, note that the function  $f$  can be related to  $x$  by deriving

$$f = A_f \cos \varphi \sin (\Omega_f t) - A_f \sin \varphi \cos (\Omega_f t) ,$$

from (3), and noting that

$$s x = A \Omega_f \cos (\Omega_f t),$$

one finally has

$$f = \frac{A_f}{A} \left( \cos \varphi - \frac{\sin \varphi}{\Omega_f} s \right) x.$$

By substituting this expression of  $f$  into equation (1), one obtains

$$[B(s) - H(s) \frac{A_f}{A} \left( \cos \varphi - \frac{\sin \varphi}{\Omega_f} s \right)] x + C(s) F(x, s x) = 0 .$$

Therefore, the nonhomogeneous differential equation (1) is reduced to a homogeneous one. by knowing the forcing function  $f = f(t)$  and by assuming the form of the solution  $x = x(t)$ . To determine the amplitude  $A$  and the phase-shift  $\varphi$  of the solution  $x(t)$ , the methods for the analysis of symmetrical self-excited oscillations as outlined in [1-3] can be used with minor modifications.

The nonlinearity  $F(x, sx)$  can be harmonically linearized as

$$F(x, sx) = N_1 x + \frac{N_2}{\Omega_f} sx$$

where the coefficients  $N_1 = N_1(A, \Omega_f)$  and  $N_2 = N_2(A, \Omega_f)$  are the describing function coefficients,

$$N_1 = \frac{1}{\pi A} \int_0^{2\pi} F(A \sin \phi, A \Omega_f \cos \phi) \sin \phi d\phi$$

$$N_2 = \frac{1}{\pi A} \int_0^{2\pi} F(A \sin \phi, A \Omega_f \cos \phi) \cos \phi d\phi$$

and  $\phi = \Omega_f t$ . The standard tables of reference [16] may be used for calculating  $N_1$  and  $N_2$ .

The linearized differential equation has the form

$$[B(s) - H(s) \frac{A_f}{A} (\cos \varphi - \frac{\sin \varphi}{\Omega_f} s) + C(s) (N_1 + \frac{N_2}{\Omega_f} s)]x = 0 \quad (4)$$

and the corresponding characteristic equation is

$$B(s) - H(s) \frac{A_f}{A} (\cos \varphi - \frac{\sin \varphi}{\Omega_f} s) + C(s) (N_1 + \frac{N_2}{\Omega_f} s) = 0 \quad (5)$$

The periodic solution  $x = A \sin(\Omega_f t)$  with the frequency  $\Omega_f$  can be determined from (5) by substituting  $s = j\Omega_f$  and using the condition that the summation of reals and imaginaries must go to zero independently.

Thus, by certain simple algebraic manipulations, one obtains

$$B_1 A - H_1 A_f \cos \varphi - H_2 A_f \sin \varphi + C_1 A N_1 - C_2 A N_2 = 0$$

$$B_2 A + H_1 A_f \sin \varphi - H_2 A_f \cos \varphi + C_1 A N_2 + C_2 A N_1 = 0$$

(6)

where  $B_1 = B_1(\Omega_f)$ ,  $B_2 = B_2(\Omega_f)$ , etc., are given as

$$B_1 = \sum_{k=0}^n b_k X_k, \quad B_2 = \sum_{k=0}^n b_k Y_k, \quad \text{etc.}$$

The functions  $X_k$  and  $Y_k$  are calculated using the recurrence relationships [see reference 26]

$$X_{k+1} + \Omega^2 X_{k-1} = 0$$

$$Y_{k+1} + \Omega^2 Y_{k-1} = 0$$

where  $X_0 \equiv 1$ ,  $X_1 \equiv 0$ ,  $Y_0 \equiv 0$ ,  $Y_1 \equiv \Omega$ . Due to the above recurrence

relationships, the  $\zeta = 0$  curve which determines the stability region in the parameter plane [1,2], can be readily plotted using a general digital computer program for n-th order characteristic polynomials.

By denoting

$$\alpha = A_f \cos \varphi \tag{7}$$

$$\beta = A_f \sin \varphi$$

equations (6) may represent two equations in two unknowns,  $\alpha$  and  $\beta$  which can be solved for  $\alpha$  and  $\beta$  as

$$\alpha = -A \frac{H_1(B_1 + C_1 N_1 - C_2 N_2) + H_2(B_2 + C_1 N_2 + C_2 N_1)}{H_1^2 + H_2^2} \tag{8}$$

$$\beta = A \frac{H_1(B_2 + C_1 N_2 + C_2 N_1) - H_2(B_1 + C_1 N_1 - C_2 N_2)}{H_1^2 + H_2^2}$$

In the  $\alpha\beta$ -plane, equations (8) may be interpreted as equations of the  $\zeta = 0$  curve as defined in reference [2]. The solution procedure starts with the plotting of a family of  $\zeta = 0$  curves for different values of the frequency  $\Omega_f$  appearing in the coefficients,  $B_1, B_2, C_1, C_2, H_1, N_1$  and  $N_2$  of (8). The unknown amplitude  $A$ , which enters both explicitly and as an argument of  $N_1$  and  $N_2$  in (8), is interpolated along the  $\zeta = 0$  curves. The loci of the point  $M(\alpha = A_f \cos \varphi ; \beta = A_f \sin \varphi)$  are concentric circles with a radius  $A_f$  and the phase-shift  $\varphi$  interpolated along the circles. Once the  $\zeta$  and  $M$ -point loci are plotted in the  $\alpha\beta$ -plane, the amplitude  $A$ , frequency  $\Omega_f$  and the phase-shift  $\varphi$  of the possible periodic solution  $x = A \sin(\Omega_f t)$  are determined at their intersections. The stability of the periodic solutions is determined graphically from the obtained plot in a straightforward manner as shown in the following example\*.

Consider a control system with the block diagram shown on Fig. 1. The related differential equation has the form

$$s(s+0.5)(s+2)(s+10)x + 10(s+1)F(x) = s(s+0.5)(s+2)(s+10)f \quad (9)$$

where the variable  $x = x(t)$  represents the error signal  $e(t)$ , and the forcing function  $f = f(t)$  is the input  $r(t)$ .

For the sinusoidal input function  $r(t) = A_f \sin(\Omega_f t - \varphi)$  the characteristic equation of the corresponding linearized system is

$$s(s+0.5)(s+2)(s+10) \left[ A - A_f \left( \cos \varphi - \frac{\sin \varphi}{\Omega_f} s \right) \right] + 10(s+1) AN_1(A) = 0 \quad (10)$$

---

\* This example has been treated analytically in reference [13] whereby, for every set of values  $(A_f, \Omega_f)$ , at least one transcendental equation has to be solved.



where the solution  $e(t)$  of equation (9) is assumed as  $e(t) = A \sin(\Omega_f t)$ .

After the substitution

$$\alpha = A_f \cos \varphi, \quad \beta = A_f \sin \varphi$$

and  $s = j\Omega_f$  into equation (10), one obtains the equation (8) of the  $\zeta = 0$  curve as

$$\alpha = \alpha(A, \Omega_f)$$

$$\beta = \beta(A, \Omega_f)$$

For the specific equation (10), equation (7) of the M-point loci and equations (8) of the  $\zeta = 0$  curve are plotted on Fig. 2 for different values of the amplitude  $A_f$  and the frequency  $\Omega_f$ , respectively, as family parameters.

The diagram of Fig. 2 is interpreted in the usual manner. For example, if the amplitude and frequency of the forcing signal  $f(t)$  are  $A_f = 5$  and  $\Omega_f = 2$ , then the related point is  $M_0$  for which the periodic solution  $x(t)$  has the amplitude  $A = 9.3$  and the phase-shift  $\varphi = 19^\circ$ .

It is of particular significance to note that if the frequency  $\Omega_f$  is increased up to  $\Omega_f = 1.4$  rad/sec, and keeping  $A_f = 5$ , the same M locus intersects the  $\zeta = 0$  curve at three points,  $M_1$ ,  $M_2$ , and  $M_3$ , which corresponds to three different periodic solutions with the same frequency  $\Omega_f = 1.4$  rad/sec. This is due to the so-called jump resonance which can be better understood by plotting the frequency response characteristics from the diagram of Fig. 2.

In Fig. 3, the closed-loop frequency response relating the input and output of the system under investigation is plotted by an analog computer for the input amplitude  $A_f = 5$ . The jump resonance is indicated in between the frequencies  $\Omega_f = 1$  and  $\Omega_f = 2$ . When the frequency,  $\Omega_f$  of the input signal is

gradually increased, the first part Oab of the gain curve  $\frac{C}{R}(j\Omega_f)$  is obtained on Fig. 3. When the frequency  $\Omega_f$  is increased at the point b, the system output changes abruptly reaching the point c. With a further increase in the input frequency, the continuous part cd is obtained. If the procedure is reversed and the frequency is decreased gradually from a higher value, the part dcb' of the gain curve is plotted. When the point b' is reached, a decrease in  $\Omega_f$  causes the output amplitude to drop discontinuously to the point a and then follows the part a0 as the frequency  $\Omega_f$  decreases to zero. The corresponding phase characteristic follows the discontinuous jumps in the amplitude as shown in the same Fig. 3.

The three points 1, 2, 3 on the gain characteristic of Fig. 3 correspond to the points  $M_1, M_2, M_3$  in the diagram of Fig. 2. The lower point 1 and the point 2 is unstable and is not observed in the system simulations or experiments. The jump resonance obtained by the computer, checks the results available on the diagram of Fig. 2. For example, the  $\zeta = 0$  curve for  $\Omega_f = 1.3$  is tangent to the M locus plotted for  $A_f = 5$ . This corresponds to the points a and b'. By interpolating between the  $\zeta = 0$  curves plotted for  $\Omega_f = 1.4$  and  $\Omega_f = 1.5$ , the frequency of the jump bc can be evaluated. (Note that the diagram of Fig. 2 relates the input  $r(t)$  and the error signal  $e(t)$ , while the plot of Fig. 3 relates  $r(t)$  and the output  $c(t)$ . This is of no essential importance since relationship  $e = r - c$  holds.)

Another observation of the jump resonance can be made if the input frequency is held constant but the input amplitude is varied so that  $A_f$  varies while  $\Omega_f$  is constant. By using again the diagram of Fig. 2, it is not difficult to show that if  $\Omega_f$  is chosen to be 1.4 and  $A_f$  is varied, a diagram of Fig. 4 can be calculated from that of Fig. 2. Once again there is a range of values

of  $A_f$  for which three values of  $A$  are possible. For  $A_f = 5$ , there are three values,  $A_1, A_2, A_3$ , of the amplitude  $A$  which correspond to the three points  $M_1, M_2, M_3$  of Fig. 2. The lower  $A_1$  and upper  $A_3$  correspond to stable solutions, while  $A_2$  is unstable and cannot be obtained experimentally. The corresponding phase diagram is shown in Fig. 5.

It is of interest to note that all diagrams of Figs. 3, 4 and 5 are obtained for specific values of either the amplitude  $A_f$  (Fig. 3,  $A_f = 5$ ) or the frequency  $\Omega_f$  (Figs. 4 and 5,  $\Omega_f = 1.4$ ). If these values are changed, all the diagrams have to be replotted again since they cannot be normalized with respect to the input as is possible in linear systems. The effects on  $(A, \varphi)$  of changing  $(A_f \Omega_f)$ , however, can be studied directly from the diagram of Fig. 2. Furthermore, the presented procedure can be applied equivalently to single-valued and common multi-valued nonlinearities as well as to nonlinearities with the frequency-dependent describing functions. In certain cases, the procedure can be extended to the analysis of the jump phenomena in nonlinear systems with two nonlinearities provided the applicability conditions of the describing function are satisfied.

#### Stability and Sensitivity of the Periodic Solutions.

In general, the jump phenomena can be more complex than that examined in the previous section. It may contain more than one curl and, thus, more than three periodic solutions are possible. After these solutions are determined, the stability problem arises to separate the stable from the unstable solutions.

The unstable solutions are related to the case when an increase in the input amplitude  $A_f$  results in a decrease of the amplitude  $A$  of the corresponding periodic solution. By examining Fig. 4, one may conclude that the

unstable solution amplitudes are located along the part of the curve for which the slope is negative. The stability can now be checked from the parameter plane diagram. So, for an increase in the amplitude  $A$  along the curve  $\Omega_f = 1.4$  at the point  $M_1$ , there is an increase in the amplitude  $A_f$ , and the related solution is stable. The same reasoning reveals that the point  $M_2$  is unstable, but  $M_3$  is again stable.

The stability of periodic solutions can be checked analytically by determining the sign of the derivative  $\partial A / \partial A_f$ . This derivative is calculated from equations 6 for the case when the frequency  $\Omega_f$  is considered constant and the amplitude  $A$  and phase  $\varphi$  are assumed to be functions of the amplitude  $A_f$ . This is quite similar to the procedure of the sensitivity analysis of self-excited nonlinear oscillations presented in reference [3]. Thus, it is left to the reader to derive the derivatives  $\partial A / \partial A_f$  and  $\partial \varphi / \partial A_f$  from equations 6; then, to apply the obtained expressions to the system investigated in the preceding section.

Likewise, the sensitivity analysis is related to the stability problem and the concept of sensitivity analysis of small parameter variations in self-excited oscillations developed in reference [3] can be extended to the forced oscillations. The coefficients of the polynomials  $B(s)$ ,  $C(s)$ , and  $H(s)$  in the characteristic equation

$$B(s) - H(s) \frac{A_f}{A} \left( \cos \varphi - \frac{\sin \varphi}{\Omega_f} \right) + C(s) \left( N_1 + \frac{N_2}{\Omega_f} s \right) = 0 \quad (5)$$

can be considered as functions of  $\mu$  linear parameters  $q_i$ , ( $i = 1, 2, \dots, \mu$ ). The describing function  $N = N_1 + jN_2$  can be considered as a function of  $A$ ,  $\Omega_f$ , and  $\nu$  nonlinear parameters  $p_j$ , ( $j = 1, 2, \dots, \nu$ ). Then the sensitivities

$$S_{q_i}^A \triangleq \frac{\partial \ln A}{\partial \ln q_i}, \quad S_{q_i}^\varphi \triangleq \frac{\partial \ln \varphi}{\partial \ln q_i}$$

$$S_{p_j}^A \triangleq \frac{\partial \ln A}{\partial \ln p_j}, \quad S_{p_j}^\varphi \triangleq \frac{\partial \ln \varphi}{\partial \ln p_j}$$

can be calculated by differentiating equations (6) with respect to either  $q_i$  or  $p_j$ . The obtained sensitivity values indicate how the steady-state values of the amplitude  $A$  and phase  $\varphi$  are affected by the small parameter variations.

It is of interest to note that the possibility of the jump resonance to take place can be indicated by the condition that the derivative  $\partial A / \partial A_f = \infty$ ; i.e.,  $\partial A_f / \partial A = 0$ . This condition has been examined entirely in references [16,17] whereby a graphical procedure has been proposed to check the condition being satisfied. The procedure of reference [17] is convenient for adjusting the linear part of the system so that jump resonance is avoided either entirely or for some range of input amplitudes.

Variation of Nonlinear Characteristic.

In the case of single-valued nonlinear characteristics when the nonlinear differential equation has the form

$$B(s)x + C(s) F(x) = H(s)f$$

and the forcing function  $f = f(t)$  is

$$f(t) = A_f \sin(\Omega_f t - \varphi) \tag{2}$$

the analysis of the periodic solution  $x = x(t)$ .

$$x(t) = A \sin(\Omega_f t) \tag{3}$$

can be performed by a different approach proposed by Gibson [19]. This approach is convenient for the analysis of the effects on jump resonance of varying the nonlinear characteristic; i.e., the nonlinear parameters. Moreover, the approach can be advantageous in cases when the nonlinear single-valued characteristic is found experimentally and the describing function is determined graphically. Of course, it may be applied to situations when the describing function of the nonlinearity is plotted experimentally or by using computers. The approach will be generalized by the parameter plane concept.

To describe the approach, note that the same harmonic linearization presented in the preceding section if applied to equation (10) yields

$$[B(s) + H(s) \frac{A_f}{A} (\cos \varphi - \frac{\sin \varphi}{\Omega_f} s) + C(s) N_1]x = 0 \quad (11)$$

where  $N_1 = N_1(A)$ . Equation (11) can be obtained from equation (4) by assuming  $N_2 \equiv 0$ , which is true for a single-valued nonlinearity  $F(x)$ .

The corresponding characteristic equation can be written as

$$B(s)A + C(s) A N_1 + H(s) A_f (\cos \varphi - \frac{\sin \varphi}{\Omega_f} s) = 0 \quad (12)$$

After substituting  $s = j\Omega_f$  into (12), one obtains two equations in two unknowns,  $\alpha$  and  $\beta$ . Thus,

$$\begin{aligned} B_1 \alpha + C_1 \alpha \beta + H_1 A_f \cos \varphi + H_2 A_f \sin \varphi &= 0 \\ B_2 \alpha + C_2 \alpha \beta - H_1 A_f \sin \varphi + H_2 A_f \cos \varphi &= 0 \end{aligned} \quad (13)$$

where

$$\alpha = A$$

$$\beta = N_1(A)$$

Equation (13) can be solved for  $\alpha$  and  $\beta$  to obtain

$$\frac{\alpha}{A_f} = \frac{(C_2 H_1 - C_1 H_2) \cos \varphi + (C_2 H_2 + C_1 H_1) \sin \varphi}{B_2 C_1 - B_1 C_2} \quad (14)$$

$$\beta = \frac{(B_1 H_2 - B_2 H_1) \cos \varphi - (B_2 H_2 + B_1 H_1) \sin \varphi}{(C_2 H_1 - C_1 H_2) \cos \varphi + (C_2 H_2 + C_1 H_1) \sin \varphi}$$

Now, for a given value of the forcing input frequency  $\Omega_f$ , the coefficients  $B_1, B_2, C_1, C_2, H_1$ , and  $H_2$ , which are functions of  $\Omega_f$  only, are evaluated numerically. For different values of the phase shift  $\varphi$ , the corresponding values  $\alpha$  and  $\beta$  are calculated from (14). Thus a locus with constant frequency  $\Omega_f$  can be plotted in the  $\alpha\beta$  plane where the scale factor along the  $\alpha$  axis is given by  $A_f$ . On the other hand, the M locus is simply the describing function curve itself. Any change in the nonlinear parameters affects only the M locus while any change in the  $A_f$  input amplitude simply effects the scale along the  $\alpha$  axis of the  $\alpha\beta$  plane for the M locus only.

To illustrate the analysis procedure, consider the same example of the previous section. Applying the outlined procedure, one obtains the parameter plane diagram shown in Fig. 6. The diagram is plotted for  $A_f = 5$  and, therefore, it can be compared with the computer simulation diagram of Fig. 3 to indicate the accuracy. The points 1, 2, 3 of the intersections of the M locus with the  $\Omega_f = 1.4$  correspond to the points 1, 2, 3 of Fig. 3. The corresponding values of the phase shift  $\varphi$  are read on the  $\Omega_f$  curves.

Any change in the amplitude  $A_f$  can be interpreted merely as a shift of the  $M$  locus relative to the  $\Omega_f$ -constant curves of Fig. 6. Thus, a slight modification of the  $M$  locus should be made each time the amplitude  $A_f$  is changed.

### Conclusions.

It has been shown that forced nonlinear oscillations, and in particular the jump resonance phenomena may be conveniently considered using the parameter plane concept. Either a parameter plane may be plotted for a specified nonlinearity and the effects of varying the forcing signal amplitude and frequency may be considered, or a parameter plane may be plotted such that the effects of varying the nonlinear characteristic may be investigated at the expense of ease of interpretation for input amplitude changes. The advantage of using the parameter plane approach is that the required design information is given conveniently on the one diagram.

The method can be extended directly to the analysis of subharmonic resonance by using the dual-input describing function as proposed by West [15].



REFERENCES

1. Siljak, D.D., "Analysis and Synthesis of Feedback Control Systems in the Parameter Plane", Pt. I - Linear Continuous Systems; Pt. II - Sampled-Data Systems; Pt. III - Nonlinear Systems, IEEE Transactions on Applications and Industry, Nov., 1964, pp 458-473.
2. Siljak, D.D., "Generalization of the Parameter Plane Method", IEEE Transactions on Automatic Control", vol. AC-11, Jan., 1966, pp 63-70.
3. Siljak, D.D., and M. R. Stojić', "Sensitivity Analysis of Self-Excited Nonlinear Oscillations", IEEE Transactions on Automatic Control, vol. AC-10, Oct., 1965, pp 413-420.
4. Siljak, D.D., "Analysis of Asymmetrical Nonlinear Oscillations in the Parameter Plane", IEEE Transactions on Automatic Control, vol. AC-11, April, 1966, pp 239-247.
5. Bogoliubov, N.N., and U. A. Mitropolsky, "Asymptotical Methods in the Theory of Nonlinear Oscillations", (in Russian), Fizmatgiz, 1963. (English Trans., Delhi, India: Hindustan Pub. Co., USA Dist.: Gordon and Breach Sci. Pub., New York).
6. Cunningham, W.J., "Introduction to Nonlinear Analysis", McGraw-Hill Book Co., Inc., New York, 1958.
7. Hayashi, Ch., "Oscillations in Physical Systems", McGraw-Hill Book Co., Inc., New York, 1964.
8. Levinson, E., "Some Saturation Phenomena in Servomechanisms with Emphasis on the Tachometer Stabilized System", AIEE Trans., vol. 72, pt II (Applications and Industry), March, 1953, pp 1-9.
9. Prince, L.T., Jr., "A Generalized Method for Finding the Closed-loop Frequency Response of Nonlinear Systems", AIEE Trans., vol. 73, pt II (Applications and Industry), Sept., 1954, pp 217-224.
10. West, J.C., J.L. Douce, and R.K. Livesley, "The Dual-input Describing Function and Its Use in the Analysis of Nonlinear Feedback Systems", IEE Proc., vol. 103, B, 1956, pp 463-474.
11. Ogata, K., "An Analytic Method for Finding the Closed-loop Frequency Response of Nonlinear Feedback-control Systems", AIEE Trans., vol. 76, pt II (Applications and Industry), Nov., 1957, pp 277-285.
12. Stein, W.A., and G.J. Thaler, "Obtaining the Frequency Response Characteristic of a Nonlinear Servomechanism for an Amplitude- and Frequency-sensitive Describing Function", AIEE Trans., vol. 77, pt II (Applications and Industry), May, 1958, pp 91-96.

13. Hopkin, A.M., and K. Ogata, "An Analytic Frequency Response Solution for a Higher Order Servomechanism with a Nonlinear Control Element," J. of Basic Engr., ASME Trans., Series D. vol. 81, March, 1959, pp 41-45.
14. Popov, E.P., and Palitov, "Approximate Methods for Analyzing Nonlinear Automatic Systems, (in Russian), Fizmatgiz, Moscow, 1960. (English trans. Foreign Tech. Div., AFSC, Wright-Patterson Air Force Base, Ohio, Rept. FTD-TT-62-910.)
15. West, J.C., "Analytical Techniques for Nonlinear Control Systems," D. Van Nostrand Co., Inc., Princeton, New Jersey, 1960.
16. Gille, J.C., and P. Decaulne, "On the Forcing Oscillations of Nonlinear Servosystems," (in French), Automatic and Remote Control, Butterworth London, vol. 1, 1961, pp 205-210.
17. McAllister, A.S., "A Graphical Method for Finding the Frequency Response of Nonlinear Closed-loop Systems, AIEE Trans., vol. 80, pt II (Applications and Industry), Nov. 1961, pp 268-277.
18. Hatanka, H., "The Frequency Response and Jump-resonance Phenomena of Nonlinear Feedback Control Systems, J. of Basic Engr., ASME Trans., Series D, vol. 85, June, 1963, pp 236-242.
19. Gibson, J.E., "Nonlinear Automatic Control," McGraw-Hill Book Co., Inc., New York, 1963.
20. Fukuma, A., and M. Matsubara, "Jump Resonance Criteria of Nonlinear Control Systems," (to be published in IEEE Trans. on Automatic Control).
21. Sagirow, P., "On the Problem of Error Estimation in the Harmonic Balance," (in German), Z. Angew. Math und Mech., Nr. 10-11, 1960.
22. Garber, E.D., "An Estimate of the Error of the Harmonic Balance Method," (in Russian) Automatika i telemekhanika, t. 24, No. 4, April, 1963, pp 482-492.
23. Sandberg, I.W., "On the Response of Nonlinear Control Systems to Periodic Input Signals," The Bell System Technical Journal, vol. 28, No. 3, May 1964, pp 911-927.
24. Garber, E.D., and E.N. Rozenvasser, "The Investigation of Periodic Regimes of Nonlinear Systems on the Basis of the Filter Hypothesis," (in Russian), Automatiki i telemekhanika, t. 26, No. 2, Feb., 1965, pp 277-287.
25. Booton, R.C., Jr., "The Analysis of Nonlinear Control Systems with Random Inputs," Proceedings of the Symposium on Nonlinear Circuit Analysis, New York, Polytechnic Institute of Brooklyn, 1953, pp 369-391.

26. <sup>v</sup>Siljak, D.D., "A Note on the Generalized Nyquist Criterion", IEEE Transactions on Automatic Control, vol. AC-11, No. 2, April, 1966, pp 317.

## List of Symbols

$s$	Differential operator
$B(s), C(s), H(s)$	Polynomials in $s$
$t$	time
$x$	input to the nonlinear element
$F(x, sx)$	nonlinear function
$f(t)$	forcing function
$A_f$	amplitude of the forcing function
$\Omega_f$	frequency of the forcing function
$\varphi$	phase shift
$A$	amplitude of the periodic solution
$N$	describing function
$N_1$	real part of the describing function
$N_2$	imaginary part of the describing function
$\phi$	phase
$X_k, Y_k$	specific functions
$\zeta$	relative damping coefficient
$\alpha, \beta$	parameters
$S_{q_i}^A, S_{q_j}^A, S_{p_i}^A, S_{p_j}^A$	sensitivities

LIST OF CAPTIONS

Fig. 1. System block diagram

Fig. 2. Parameter plane diagram

Fig. 3. Frequency response

Fig. 4. Amplitude diagram

Fig. 5. Phase diagram

Fig. 6. Parameter plane diagram

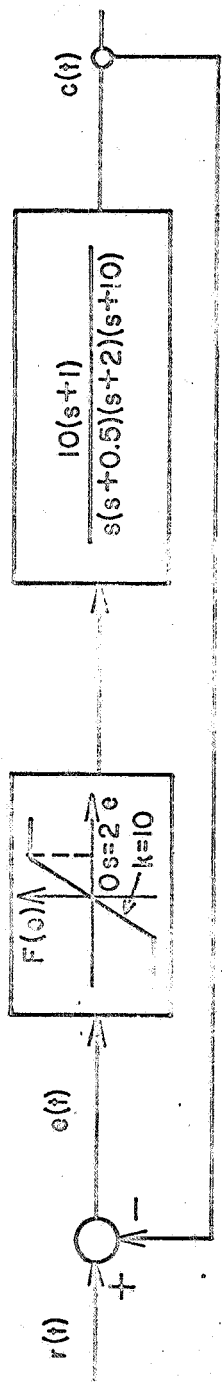


FIG. 1

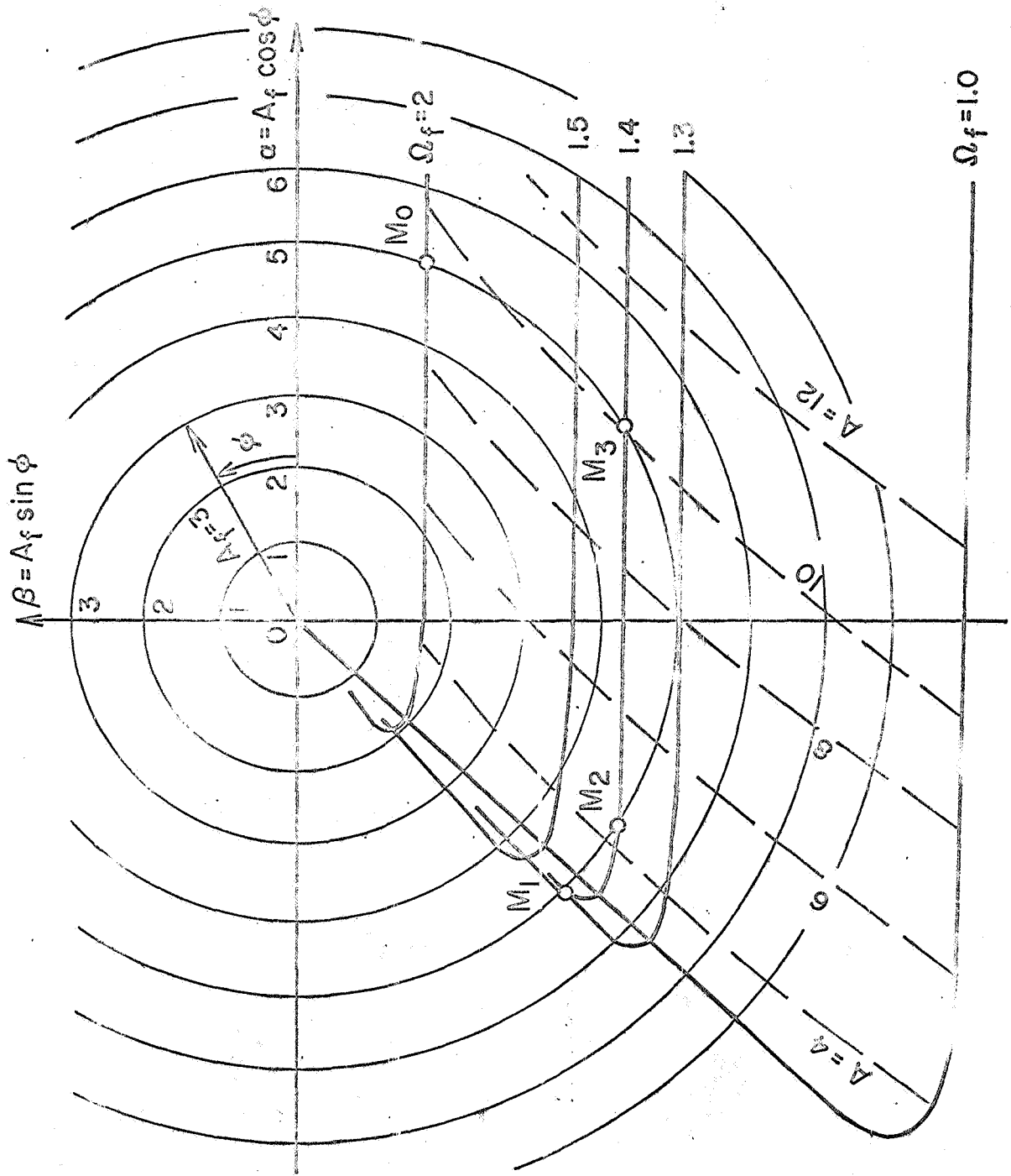


FIG. 2

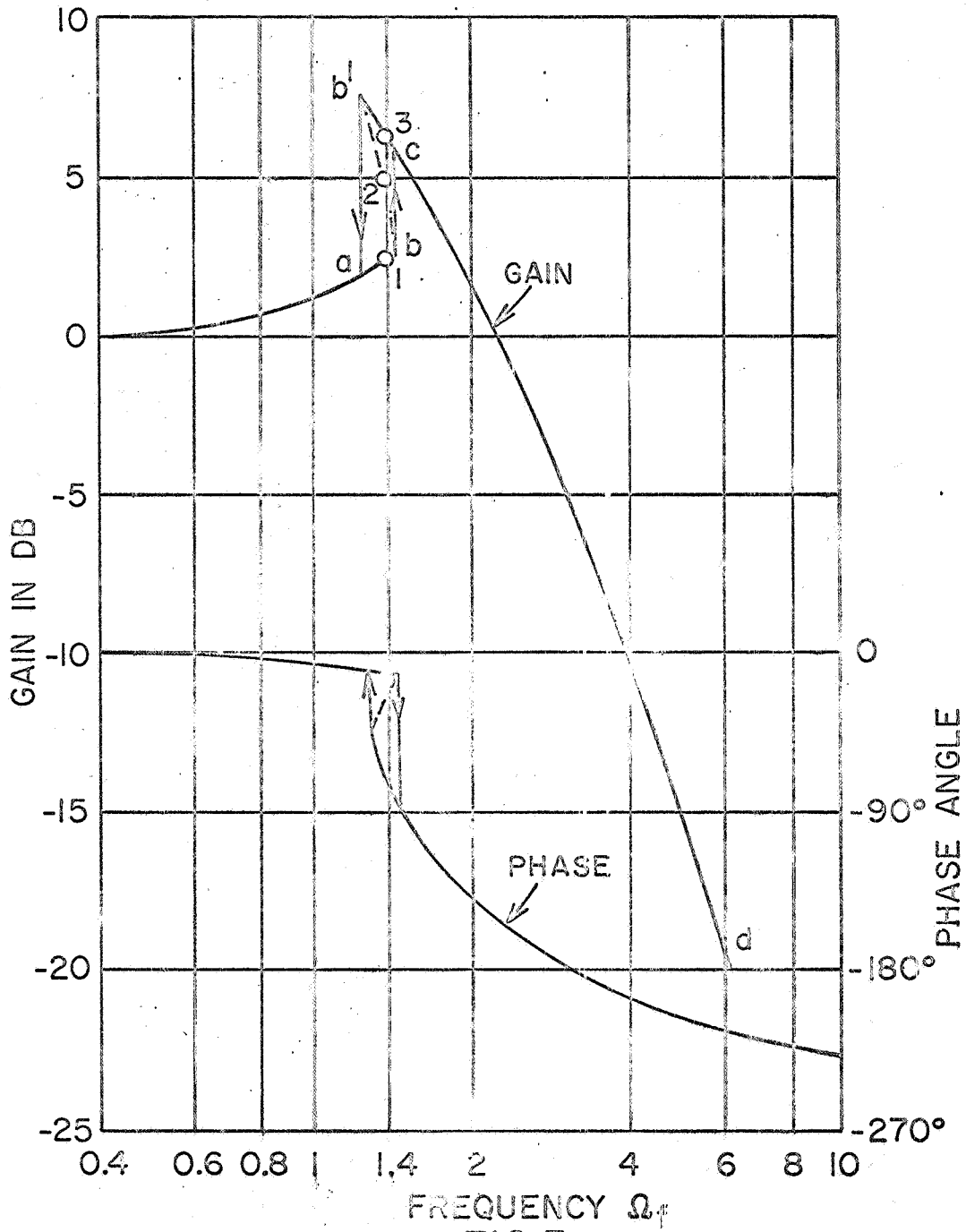


FIG.3



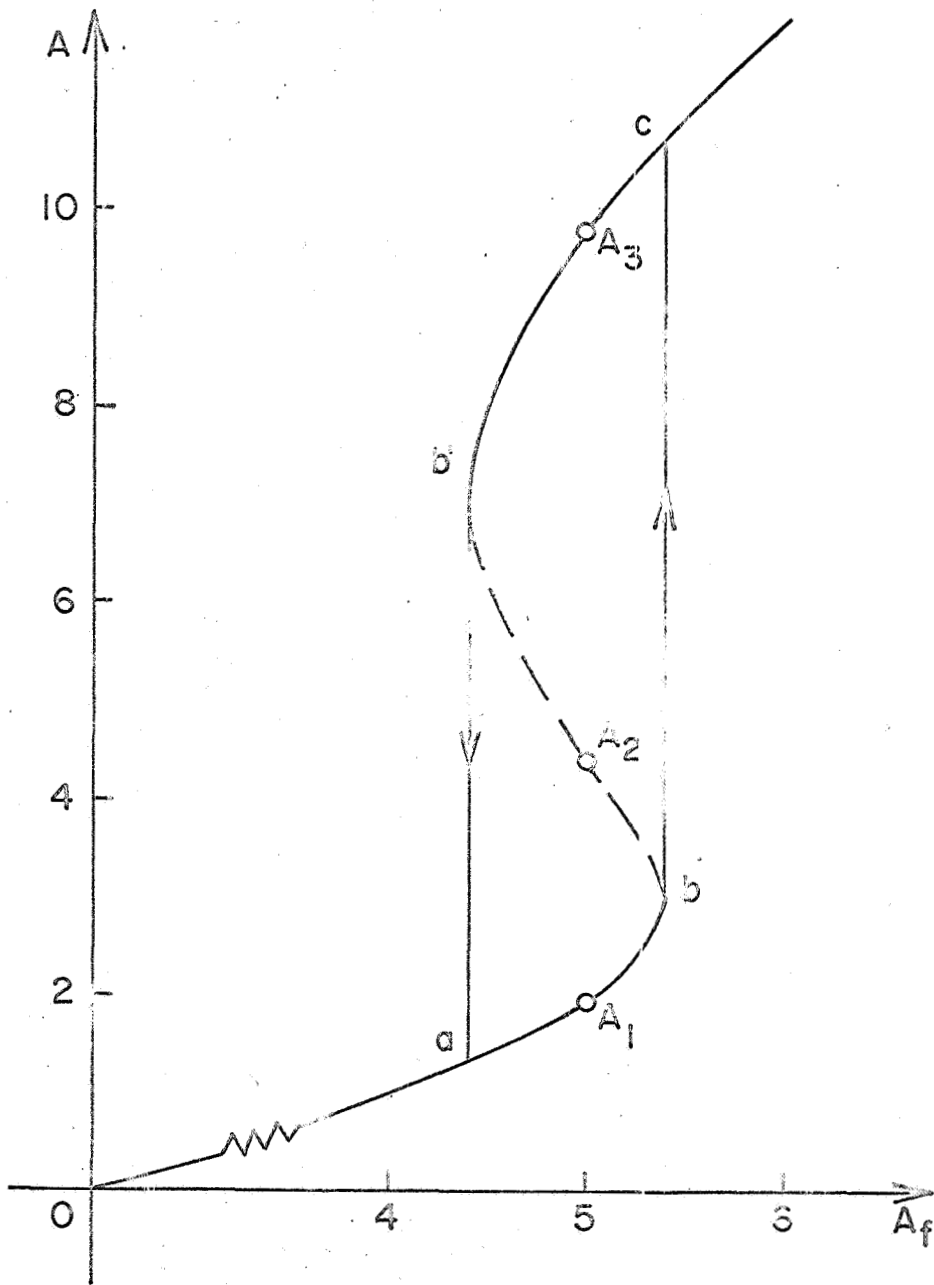


FIG. 4

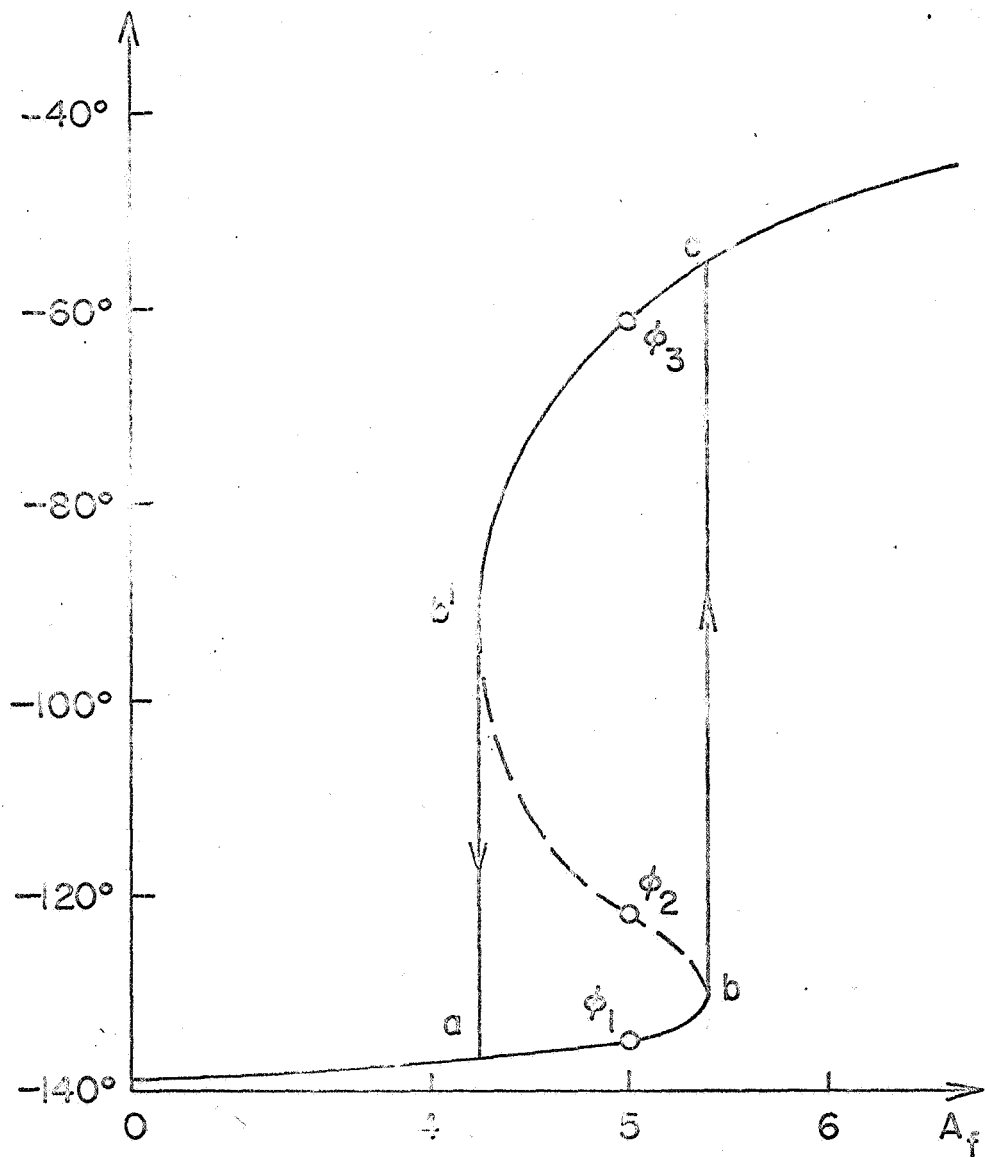


FIG. 5

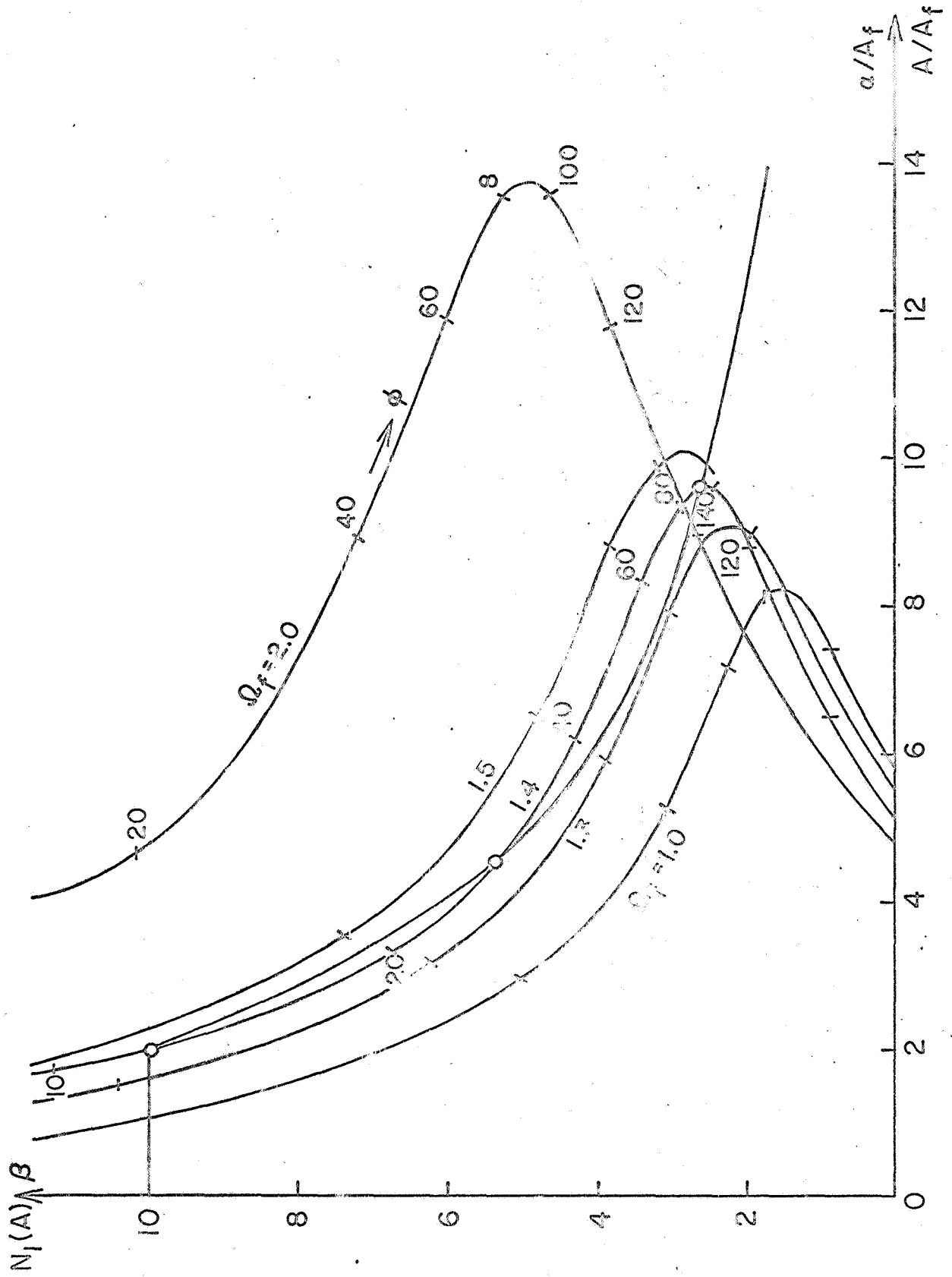


FIG. 6